Simulations of the Temperature Dependence of Amide I Vibration

Jakub Kaminský,*,†,‡ Petr Bouř,‡ and Jan Kubelka*,†

University of Wyoming, 1000 East University Avenue, Laramie, Wyoming 82071, United States, and Institute of Organic Chemistry and Biochemistry, Academy of Sciences, 166 10 Prague, Czech Republic

Received: September 6, 2010; Revised Manuscript Received: November 15, 2010

For spectroscopic studies of peptide and protein thermal denaturation it is important to single out the contribution of the solvent to the spectral changes from those originated in the molecular structure. To obtain insights into the origin and size of the temperature solvent effects on the amide I spectra, combined molecular dynamics and density functional simulations were performed with the model *N*-methylacetamide molecule (NMA). The computations well reproduced frequency and intensity changes previously observed in aqueous NMA solutions. An empirical correction of vacuum frequencies in single NMA molecule based on the electrostatic potential of the water molecules provided superior results to a direct density functional average obtained for a limited number of solute−solvent clusters. The results thus confirm that the all-atom quantum and molecular mechanics approach captures the overall influence of the temperature dependent solvent properties on the amide I spectra and can improve the accuracy and reliability of molecular structural studies.

I. Introduction

Structural changes in peptides and proteins upon thermal denaturation are conveniently studied with the aid of infrared spectroscopy (IR). Most commonly, the amide I band (mostly C═O bond stretching, Figure 1) is used as a sensitive probe of the secondary structure and structural changes. Amide I frequencies and band shapes are characteristic for α-helical, coil, or pleated sheet peptide forms.[1,2] However, the interpretation of the temperature-dependent amide I spectra in aqueous solution is complicated by nonstructural effects, in particular the frequency shifts and intensity changes due to the surrounding solvent medium.[3] Understanding nonstructural media effects in IR spectroscopy is thus necessary for correct interpretation of the experimental data in terms of protein structures or structural transitions.

Numerous theoretical and experimental studies have focused on the solvent effects on the amide I vibrational frequencies, in particular in model compounds, such as NMA.[4,5] This molecule is perhaps too simple a model for complete polypeptide chains; nevertheless NMA became a paradigm system for amide vibrational studies. Aside from its small size, the amide spectral signals are not complicated by conformational flexibility, as in longer peptides. Since the conformational properties are also temperature dependent, they interfere with the temperature-dependent spectral properties caused by the solvation. For these reasons, NMA is a well suited model molecule for studies of the inherent temperature dependence of the amide I spectra.[6−8]

The temperature dependence of the amide vibrational spectra has so far received only limited attention. Specifically for NMA, several authors observed frequency shifts with temperature in the neat liquid.[9−12] Ludwig et al.[13] found that temperature caused frequency shifts of the amide I band in a mixture of NMA and $CHCl_3$. Naturally, aqueous solutions are the most relevant for biological applications. Manas et al.[6] recorded differences in the NMA frequencies in D_2O-based solution within 10−290 K. The frequency shifts were generally attributed to the strength of hydrogen bonding: either between NMA molecules (in $CHCl_3$) or between the NMA and the solvent (in D_2O). One of us[7,8] previously showed that hydrogen bonding is not the only cause as similar frequency shifts were observed in solvents without acidic hydrogen. On the basis of the Onsager reaction field model, the temperature dependence was explained by the solvent dielectric properties. However, the electrostatic model could not capture the NMA amide I' frequency and intensity shifts in D_2O since it does not explicitly account for the hydrogen bonding.

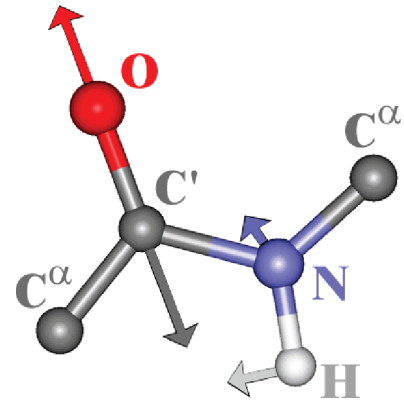

Figure 1. The *N*-methylacetamide (NMA) and the amide I vibration.

In this study, we employ a more realistic model based on combined density functional theory (DFT) and molecular dynamics (MD) calculations. As shown below, the NMA clusters with explicit water molecules can reproduce the observed temperature dependent IR spectral changes of the amide I band. The combination of the DFT vibrational parameters for the solute molecule (NMA) with the MD simulations of the solvent (water), provides means for taking into account the effects of the solvent and its dynamics at the molecular level. So far, this methodology was applied to the simulations of the amide spectra of NMA and several short peptides.[14−16] Since the temperature dependence of the IR spectra

* To whom correspondence should be addressed. E-mail: kaminskj@gmail.com (J.Kaminsky); jkubelka@uwyo.edu (J.Kubelka).
† University of Wyoming.
‡ Academy of Sciences.

10.1021/jp1084839
Published on Web 12/09/2010

has been related to the solvent properties, MD simulations of the solvent dynamics at various temperatures should be able to account for the temperature effects. Calculations of the temperature dependent IR spectra therefore represent important tests for the empirical solvent correction methodologies.

II. Methods

Periodic boxes (20 × 20 × 20 Å^3) containing 259 water molecules and NMA (Figure 1) were created by the Protein and XYZEdit programs included in the Tinker Molecular Mechanics package.[17] With the Amber99 force field[18] a classical MD of an NpT ensemble was run for 1 ns, with 1 fs integration time step, and pressure of 1 atm. The pressure was controlled with the Berendsen volume scaling barostat.[19] The simulations were run at two temperatures (273 and 353 K), approximately covering the practical experimental range.[7,8] The temperature was maintained with the Berendsen bath coupling method.[19] The TIP3P force field as a part of Amber99 was used for water molecules.

Equilibration runs were performed for 20 ps, until the size of the box (under constant pressure) stabilized. Subsequently, 10000 geometry snapshots were acquired at 0.1 ps intervals for each temperature. Radial distribution functions were calculated averaging 10000 geometries. NMA/water clusters were constructed from eighteen random snapshots, in which only water molecules within the 5 Å distance from NMA atoms were retained, resulting in clusters of NMA with three to ten water molecules. Geometries of these NMA/water clusters were partially optimized using normal mode coordinates,[20] where only high-frequency ($300 > \omega > i300$ cm^{-1}) modes were relaxed in order to preserve the overall cluster structures. Additionally, to take into account the bulk solvent, the conductorlike (CPCM) implicit solvent model was applied.[21,22] Gaussian default CPCM cavity parameters were used, i.e., simple united atom (UA) topological model and average tessera areas of 0.2 Å^2.

For the MD clusters harmonic vibrational frequencies were calculated by the Gaussian suite of programs.[23] The GGA-BPW91 DFT functional[24] with standard 6-311++G** basis set was used by default. Aqueous environment extending far from the solute was simulated by CPCM.

An alternative approach to the simulation of hydrated NMA spectra was based on an empirical correction, where the electrostatic field of surrounding water molecules perturbs the vacuum frequencies and intensities. This approach, often referred to as the "electrostatic map", allows to incorporate the effects of large number (thousands) of solvent molecules as well as their dynamical fluctuations. Details of the theory are described elsewhere,[15,16] and only a brief summary will be presented here.

The electrostatic map model is based on an empirical linear relationship between the vibrational force constants and intensity parameters (transition dipole moments), and the electrostatic field due to the solvent acting on the amide group atoms. For the vibrational force field (FF)

$$\Lambda_I = \Lambda_{0I} + \sum_{j=1}^{N} b_{Ij}\varphi_j \qquad (1)$$

where Λ_{0I} is a force constant in vacuum, with the normal mode index I, $I = 1...3N$, where N is the number of atoms ($N = 4$ for the peptide HNCO group). The φ_j is the electrostatic (Coulombic) potential of the solvent measured at the atom j of the solute. The potential was calculated from partial charges of water atoms. For a better description of the electrostatic field surrounding the peptide group two α-carbons attached to the HNCO segment were considered for the potential ($N = 6$); this, however, brough minor differences only if compared to $N = 4$. The conservation condition $\sum_{j=1}^{N} b_{I_j} = 0$ ensures zero frequency shifts in the case of constant potential. This approach provided encouraging results on many systems, including NMA-water clusters or hydrated peptides.[14,15] In our case, the b_{Ij} coefficients were obtained from a set of 11 NMA−water clusters previously by a minimization of the root-mean-square differences between computed and fitted force constants.[16]

Similarly, for the Cartesian dipole derivatives P (atomic polar tensor)

$$P_{\mu\alpha,\beta} = P_{0,\mu\alpha,\beta} + \sum_{j=1}^{N} c_{j,\mu\alpha,\beta}\varphi_j \qquad (2)$$

where the α-coordinate index belongs to atom μ and β denotes the electric dipole component. To avoid the orientation dependence, local normal mode force constants were fitted in eq 1, while internal coordinate representation was used for the dipole derivatives.[15] In this manner, vibrational frequencies and dipole strengths were obtained for each of the 10000 MD snapshots. The total spectrum of the solvated NMA was then calculated as a sum over all the MD snapshots. Resulting spectral shapes were created using the Tabprn program,[25] developed in house, by assigning Gaussian-type peaks with a uniform width of 5 cm^{-1} to all transitions. To better estimate the central frequency and bandwidth of the resulting amide I IR band, the simulated absorption profile was fitted by a single Gaussian band.

To test for the effects of the solvent polarizability, which is neglected in the Amber99 force field, Amoeba polarizable force field[26] was also used with all conditions identical to those described above. Simulations with both force fields were carried out under NVT conditions in addition to NpT. Experimental amide I' spectra of NMA in D_2O at many temperatures were obtained as described in detail previously.[7,8]

III. Results and Discussion

NMA Structure and Solvation Shells. Because of the weak thermostat coupling, the temperature slightly varied during the MD simulation, which can be seen in the Supporting Information. Mean average deviations are included in Table I. For Amber99, the temperature oscillates around the desired values of 273 and 353 K, respectively. The Berendsen thermostat coupled with the Amoeba force field maintained the temperature about 13 K higher than desired. A replacement by the Andersen thermostat (Andersen stochastic collision method, Figure 1S in SI) brought only a minor improvement, and the average temperature was still by about 10 K higher. Nevertheless, the temperature difference (80 K) relevant to the experiment[7,8] was reproduced correctly by both force field models, and as all the other parameters behaved realistically, we found the Amoeba simulation suitable for the comparison.

Another parameter monitored to ensure realistic MD simulation conditions was the size of the periodic box for the NpT ensemble (see Figure 2). Initial box size was set to 20 Å on the side. For the Amber99 force field the size oscillated around 19.8 Å at the lower temperature (∼273 K) and around 20.3 Å at 353 K. The Amoeba force field yielded box sizes by about 0.4 Å smaller (Figure 2). The differences between the sizes at higher and lower temperature are approximately the same for both force fields.

TABLE I: Experimental and Simulated Amide I Spectral Parameters for NMA in Aqueous Solution

		MD correction				
		Amber99		Amoeba		
parameter[a]	experiment	NpT	NVT	NpT	NVT	DFT clusters
T_1 (K)	274	273 ± 2	273 ± 2	285 ± 2	285 ± 2	273 ± 2
T_2 (K)	357	353 ± 3	353 ± 3	367 ± 3	367 ± 3	353 ± 3
ρ_{T_1} (kg m^{-3})	1000[b]	1012	988	1070	988	
ρ_{T_2} (kg m^{-3})	972[b]	942	962	998	962	
ν_{T_1} (cm^{-1})	1621[c]	1622	1621	1620	1616	1628
ν_{T_2} (cm^{-1})	1627[c]	1626	1627	1623	1621	1630
$\Delta\nu$ (cm^{-1})	6	4	6	3	5	2
$\Delta\nu/\Delta T$ (cm^{-1}/K)	0.07[c]	0.05	0.08	0.04	0.06	0.03
D_{T_1} (10^{-2} × Debye^2)	12.1[d]	10.7	10.8	12.0	11.8	11.3
D_{T_2} (10^{-2} × Debye^2)	10.6[d]	10.5	10.4	11.4	11.3	8.0
$\Delta D/D_{T_1}$ (%)	12[d]	2	4	5	4	29
δ_{T_1} (cm^{-1})	27.9	37	32	42	39	
δ_{T_2} (cm^{-1})	27.5	46	37	45	49	

[a] Temperatures (T), densities (ρ), amide I band frequency (ν), dipole strength (D), and full width of the amide I band at half-maximum (δ). [b] Reference 32, H_2O. [c] Reference 7. [d] Reference 8.

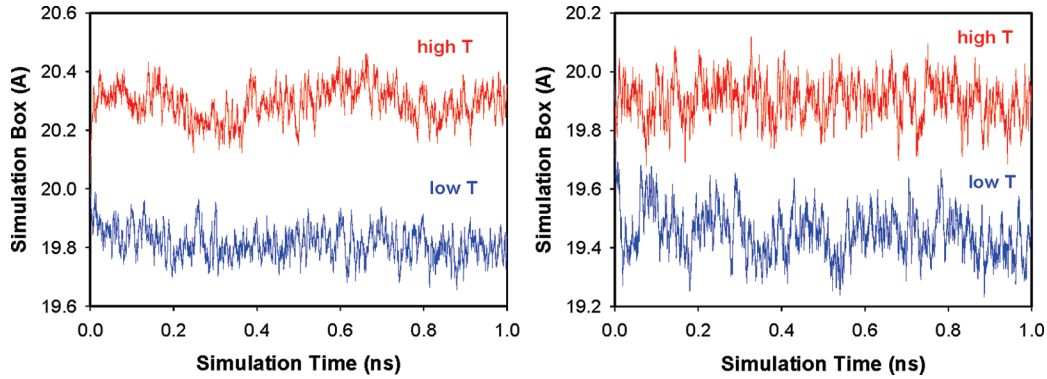

Figure 2. The simulation box dimension during the 1 ns NpT MD simulation with Amber99 (left) and Amoeba (right) force field.

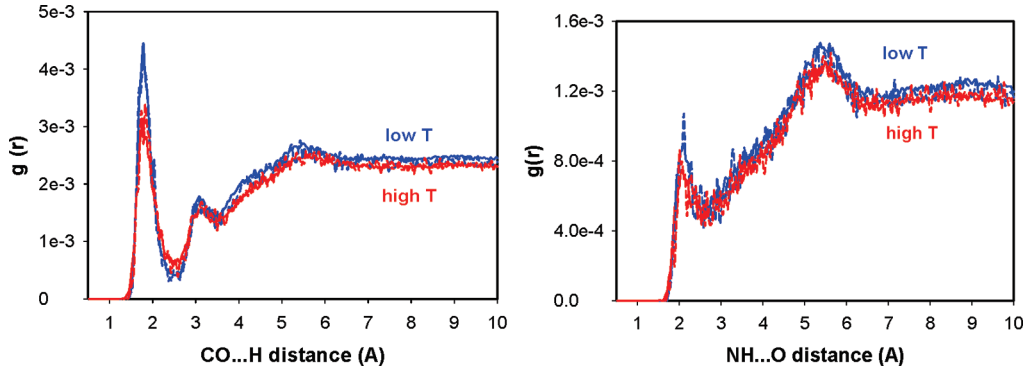

Figure 3. Radial distribution functions between water oxygen atoms and the NH hydrogen (NH···O, left) and water hydrogen atoms and the CO oxygen (CO···H, right). Both NpT (solid) and NVT (dashed) ensemble simulations are shown.

The solvation shell structure is reflected in the radial distribution functions (RDF) plotted in Figure 3. The CO···H RDF has a very sharp maximum at ~1.8 Å for both temperatures (Amber99 FF). By contrast, the NH···O distribution is much less structured. Its first maximum is at ~2.1 Å for both temperatures and less sharp than that for CO···H. Quantitatively, the RDF values of NH···O maxima are three times smaller than for the CO···H distribution. The calculated RDFs are in a good agreement with the distributions obtained previously with other MD models.[27,28]

The simulated temperature effect on RDFs is significant; the higher temperature (353 K) leads to lower maxima, by about 25%, than at 273 K. Obviously, higher temperature causes lower solute density and larger NMA−water distances. The simulated temperature dependence of RDFs approximately corresponds to that reported by Whitfield for neat NMA.[9]

Amide I Spectra. Table I summarizes main spectral characteristics of the amide I simulated for NMA−water clusters as well as for vacuum results corrected by the solvent electrostatic map. The overall amide I absorption profile obtained by the electrostatic map averaging is plotted in Figure 4. The simulated temperature shifts are smaller than the experimental value of 6 cm^{-1}, corresponding to the temperature change of 83 K.[7] For the NpT ensemble the difference was 4 and 3 cm^{-1} for the Amber99 and Amoeba force fields, respectively. For NVT, the simulated shifts of 6 (Amber99) and 5 cm^{-1} (Amoeba) were closer to the experiment. This corresponds to the average amide I frequency change in the NpT simu-

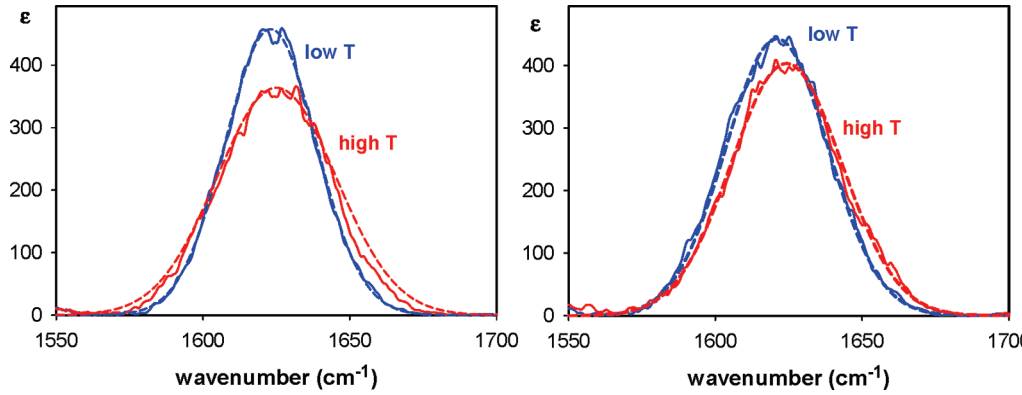

Figure 4. Simulated IR absorption profile of the amide I NMA band. For MD geometries the BPW91/6-311++G** vacuum values were corrected for the electrostatic potential of water. The MD simulations lasted 1 ns and were performed with two force fields (Amber99 - left, Amoeba - right, NpT ensemble) and two temperatures (273 and 353 K). The dashed lines show the fitted Gaussian peaks.

lation of 0.05 and 0.04 cm^{-1}/K for the Amber99 and Amoeba force field, respectively. The NVT simulations yielded slopes of 0.08 (Amber99) and 0.06 cm^{-1}/K (Amoeba); the experimental value is 0.07 cm^{-1}/K.

The direct computation on NMA-water clusters gave slightly worse results than the electrostatic map correction. The frequencies at both temperatures were higher than experiment, and the difference was too small (~2 cm^{-1}). Some of the inaccuracy can originate from the limited number of clusters (18) used for the averaging. Note that the standard errors of the average frequency are 4 cm^{-1} for lower and 5 cm^{-1} for the higher temperature, respectively, i.e., larger than the temperature shifts. The cluster values thus can be considered only approximate. Unfortunately, this procedure is very time-consuming and did not allow us to increase the number of clusters significantly.

Next, we compare relative amide I IR intensity changes to the experimental observations,[8] which revealed a 12% dipole strength decrease, from 12.1 × 10^{-2} $Debye^2$ at 274 K to 10.6 × 10^{-2} $Debye^2$ at 357 K (see Table I). All simulations with the empirical electrostatic corrections resulted in an intensity decrease of about 2−5%, somewhat lower if compared to experiment. Calculated dipole strengths at the low temperature ranged from 10.7 to 12.0 × 10^{-2} $Debye^2$, depending on particular conditions (force field, NpT, or NVT). The Amber99 predictions are substantially lower than the experimental values, while Amoeba better reproduced the experiment. By contrast, dipole strengths for the high temperature and Amber99 vary from 10.4 to 10.5 × 10^{-2} $Debye^2$, which is much closer to the experiment than for Amoeba (11.3 and 11.4 × 10^{-2} $Debye^2$). The direct NMA−water cluster approach significantly overestimated the temperature effect, as it gave a decrease in intensity of 29% (from 11.3 to 8.0 × 10^{-2} $Debye^2$).

Amide I bandwidth simulated by the empirical electrostatic correction is approximately the same for both temperatures, which corresponds to the experimental trend.[8] The absolute FWHM (full width at half maximum) values of 27.9 cm^{-1} (274 K) and 27.5 cm^{-1} (357 K) are greater than experimentally measured, as is virtually always seen in the spectra simulations using electrostatic map approach.[29,30] The NpT and NVT ensembles provided similar bandwidths for all temperatures (see Figure 4 and SI).

Relation to the Dielectric Continuum Models. Previously, the effects of solvent on NMA amide I frequencies[7] and intensities[8] were analyzed using the electrostatic model of Buckingham,[31] which incorporated the temperature dependence of the solvent dielectric constant, refractive index, and NMA density. The model very well reproduced the amide I frequencies and intensities as a function of temperature in three non-hydrogen bonding solvents (DMSO, acetonitrile, and dioxane). With the same set of parameters the prediction for NMA in D_2O fell short of the experiment, which was expected, as hydrogen bonding is not accounted for by the reaction field. Note that D_2O is used instead of H_2O experimentally, to avoid overlap of the amide I and water bending absorption bands; in our modeling we neglected the isotopic effects, presumably smaller than these caused by the temperature changes. Nevertheless, the previous models demonstrated that the solvent electrostatic properties can completely account for the amide I frequency and intensity shifts in non-hydrogen bonding solvents and for a significant part of these effects also in D_2O. It was also shown that the changes in density with temperature, approximated by the density of neat NMA, are critical for reproducing the experimental spectral shifts.[7,8]

These conclusions are consistent with the results of the present study. The temperature dependence of the calculated water RDF corresponds to that of the neat NMA and supports the idea of Amunson et al.[12] who used NMA density and its change with temperature to approximate the Onsager cavity radius. They showed that NMA has "volume" that depends on temperature and is similar in water or in the neat liquid.[7,8] The hydrogen bonding effects also seem to be well accounted for by the parametrization of the electrostatic potential correction, yielding the correct temperature dependence. (Note that the Buckingham model[7,8] did not give the correct results for D_2O because the parameters determined for the aprotic solvents were used; the data could be trivially reproduced with parameters independently adjusted for D_2O). By contrast, the direct DFT treatment of the few limited size clusters, augmented with the continuum solvent, is not sufficient to capture the bulk solvent effect, as reflected in almost negligible change in the amide I frequency. Moreover, the cluster calculations significantly overestimate the intensity change, which may be an artifact due to the limited size and number of NMA-solvent clusters.

Comparison of Force Fields and Simulation Ensembles. Several systematic differences are apparent between the simulations using two force fields: Amber99 and polarizable Amoeba. The Amoeba under the NpT conditions results in more dense solutions (1070 and 998 kg m^{-3}, respectively) than Amber99 (1012 and 942 kg m^{-3}, respectively), even if simulated temperatures were slightly higher with Amoeba (285.3 and 367.0 K, respectively) than with Amber99 (272.9 and 352.9 K). Although all densities are probably too high, Amber99 values still better reproduce the experiment. Experimental densities of water at particular temperatures can be found in the literature[32]

and are listed in Table I. By assumption of a highly diluted NMA solution, these values reasonably well agree with our calculated densities.

Interestingly, the NVT ensemble simulations are in a better correspondence with experimental densities than the NpT. The input densities for 20 Å box sizes were 988 (lower *T*) and 962 kg m^{-3} (higher *T*), respectively. The density gradients with temperature are smaller and closer to experimental values than for the NpT. If we focus only on Amber99 simulations, the NVT ensemble simulations better reproduce temperature effects on IR frequencies and dipole strengths than the NpT ones. At low temperature (273 K), whether the NVT or NpT conditions are used has only minor effect on a local water density around C═O oxygen atom, as can be seen from the radial distribution functions in Figure 3. At the high temperature (353 K) more water molecules cluster around the C═O oxygen in the NVT simulations than in the NpT.

To improve the accuracy of the simulations in the future would therefore require amelioration of many problems, such as more accurate MD force fields, more extensive cluster averaging, replacing the empirical electrostatic model by full quantum interactions, etc. Furthermore, effects of anharmonic forces go well beyond the scope of the present work. On the other hand, from the results presented above, it is clear that the combined QM/MM modeling can realistically reproduce the most important trends in the temperature dependence of the amide vibration, as well as verify the simpler continuum hydration models.

IV. Conclusions

We have investigated the temperature effects on the amide I spectra of NMA in aqueous solutions, using DFT in combination with the explicit representation of the solvent from MD trajectories at two different temperatures. The simulations based on the empirical correction of the amide I frequencies and intensities for the water electrostatic potential reproduced reasonably well the experimentally observed frequency and intensity changes with temperature. By contrast, explicit DFT calculations on the small number of NMA−water clusters extracted from the MD trajectory reproduce the experiment data only approximately, most probably due to the limited number of the clusters. Our results show that the solvent electrostatic effects are the most important factors contributing to the experimental spectral signals. Furthermore, we have verified that the temperature dependence of the solvent effects can be realistically captured by the dynamics described by the classical force fields. This study also demonstrates that temperature dependent spectral properties represent important and stringent tests for the simulation methods. Taking into account the amide I temperature correction in the simulations can significantly enhance the reliability of IR peptide structural and folding studies.

Acknowledgment. Grants of the Czech Academy of Sciences (M200550902, IAA400550702), the Grant Agency of the Czech Republic (project P208/10/P356), and the National Science Foundation (CAREER 0846140) are gratefully acknowledged.

Supporting Information Available: Figures depicting the temperature monitored during the 1-ns MD simulation and simulated IR absorption profile of the amide I NMA band. This material is available free of charge via the Internet at http://pubs.acs.org.

References and Notes

(1) Barth, A.; Zscherp, C. *Q. Rev. Biophys.* **2002**, *35*, 369.
(2) Krimm, S.; Bandekar, J. *Adv. Protein Chem.* **1986**, *38*, 181.
(3) Amunson, K. E.; Ackels, L.; Kubelka, J. *J. Am. Chem. Soc.* **2008**, *130*, 8146.
(4) Kubelka, J.; Keiderling, T. A. *J. Phys. Chem. A* **2001**, *105*, 10922.
(5) Torii, H.; Tatsumi, T.; Kanazawa, T.; Tasumi, M. *J. Phys. Chem. B* **1998**, *102*, 309.
(6) Manas, E. S.; Getahun, Z.; Wright, W. W.; Degrado, W. F.; Vanderkooi, J. M. *J. Am. Chem. Soc.* **2000**, *122*, 9883.
(7) Amunson, K. E.; Kubelka, J. *J. Phys. Chem. B* **2007**, *111*, 9993.
(8) Ackels, L.; Stawski, P.; Amunson, K. E.; Kubelka, J. *Vib. Spectrosc.* **2009**, *50*, 2.
(9) Whitfield, T. W.; Martyna, G. J.; Allison, S.; Bates, S. P.; Vass, H.; Crain, J. *J. Phys. Chem. B* **2006**, *110*, 3624.
(10) Czarnecki, M. A.; Haufa, K. Z. *J. Phys. Chem. A* **2005**, *109*, 1015.
(11) Huang, H.; Malkov, S.; Coleman, M.; Painter, P. *J. Phys. Chem. A* **2003**, *107*, 7697.
(12) Herrebout, W. A.; Clou, K.; Desseyn, H. O. *J. Phys. Chem. A* **2001**, *105*, 4865.
(13) Ludwig, R.; Reis, O.; Winter, R.; Weinhold, F.; Farrar, T. C. *J. Phys. Chem. B* **1998**, *102*, 9312.
(14) Ham, S.; Kim, J. H.; Kochan, L.; Cho, M. *J. Chem. Phys.* **2003**, *118*, 3491.
(15) Bouř, P.; Keiderling, T. A. *J. Chem. Phys.* **2003**, *119*, 11253.
(16) Bouř, P.; Michalík, D.; Kapitán, J. *J. Chem. Phys.* **2005**, *122*, 144501.
(17) Ponder, J. W. *Tinker, Software Tools for Molecular Design*; Ed. 3.8; Washington University School of Medicine: Saint Louis, 2000.
(18) Wang, J.; Cieplak, P.; Kollman, P. A. *J. Comput. Chem.* **2000**, *21*, 1049.
(19) Berendsen, H. J. C.; Postma, J. P. M.; van Gunsteren, W. F.; Dinola, A.; Haak, J. R. *J. Chem. Phys.* **1984**, *81*, 3684.
(20) Bouř, P. *Collect. Czech. Chem. Commun.* **2005**, *70*, 1315.
(21) Klamt, A.; Jonas, V.; Burger, T.; Lohrentz, J. C. W. *J. Phys. Chem. A* **1998**, *102*, 5074.
(22) Barone, V.; Cossi, M. *J. Phys. Chem. A* **1998**, *102*, 1995.
(23) Frisch, M. J.; Trucks, G. W.; Schlegel, H. B.; Scuseria, G. E.; Robb, M. A.; Cheeseman, J. R.; Montgomery, J. A., Jr.; Vreven, T.; Kudin, K. N.; Burant, J. C.; Millam, J. M.; Iyengar, S. S.; Tomasi, J.; Barone, V.; Mennucci, B.; Cossi, M.; Scalmani, G.; Rega, N.; Petersson, G. A.; Nakatsuji, H.; Hada, M.; Ehara, M.; Toyota, K.; Fukuda, R.; Hasegawa, J.; Ishida, M.; Nakajima, T.; Honda, Y.; Kitao, O.; Nakai, H.; Klene, M.; Li, X.; Knox, J. E.; Hratchian, H. P.; Cross, J. B.; Bakken, V.; Adamo, C.; Jaramillo, J.; Gomperts, R.; Stratmann, R. E.; Yazyev, O.; Austin, A. J.; Cammi, R.; Pomelli, C.; Ochterski, J. W.; Ayala, P. Y.; Morokuma, K.; Voth, G. A.; Salvador, P.; Dannenberg, J. J.; Zakrzewski, V. G.; Dapprich, S.; Daniels, A. D.; Strain, M. C.; Farkas, O.; Malick, D. K.; Rabuck, A. D.; Raghavachari, K.; Foresman, J. B.; Ortiz, J. V.; Cui, Q.; Baboul, A. G.; Clifford, S.; Cioslowski, J.; Stefanov, B. B.; Liu, G.; Liashenko, A.; Piskorz, P.; Komaromi, I.; Martin, R. L.; Fox, D. J.; Keith, T.; Al-Laham, M. A.; Peng, C. Y.; Nanayakkara, A.; Challacombe, M.; Gill, P. M. W.; Johnson, B.; Chen, W.; Wong, M. W.; Gonzalez, C.; Pople, J. A. *Gaussian 03*, revision C.02; Gaussian, Inc.: Wallingford, CT, 2004.
(24) Becke, A. *Phys. Rev. A* **1988**, *38*, 3098–3100.
(25) Bouř, P. *Spectra Simulation Freeware*; Academy of Sciences of the Czech Republic: Prague, 1998.
(26) Ren, P.; Ponder, W. *J. Phys. Chem. B* **2003**, *107*, 5933.
(27) Mennucci, B.; Martínez, J. M. *J. Phys. Chem. B* **2005**, *109*, 9818.
(28) DeCamp, M. F.; DeFlores, L.; McCracken, J. M.; Tokmakoff, A.; Kwac, K.; Cho, M. *J. Phys. Chem. B* **2005**, *109*, 11016.
(29) Grahnen, J. A.; Amunson, K. E.; Kubelka, J. *J. Phys. Chem. B* **2010**, *114*, 13011–13020.
(30) Bouř, P.; Keiderling, T. A. *J. Phys. Chem. B* **2005**, *109*, 23687.
(31) Buckingham, A. D. *Proc. R. Soc. London, Ser. A* **1958**, *248*, 169.
(32) *CRC Handbook of Chemistry and Physics*, 84 ed.; CRC Press LLC: Boca Raton, 2003.

JP1084839